THE JOURNAL OF
PHYSICAL CHEMISTRY C

Hydrogen Peroxide Generation at Liquid|Liquid Interface under Conditions Unfavorable for Proton Transfer from Aqueous to Organic Phase

Justyna Jedraszko,[†] Wojciech Nogala,[†] Wojciech Adamiak,[†] Ewa Rozniecka,[†]
Iwona Lubarska-Radziejewska,[†] Hubert H. Girault,[‡] and Marcin Opallo*,[†]

[†]Institute of Physical Chemistry, Polish Academy of Sciences, Warsaw 01-224, Poland
[‡]LEPA, Ecole Polytechnique Federale de Lausanne, Lausanne CH-1015, Switzerland

Supporting Information

ABSTRACT: The charge transfer processes across the interface between two immiscible electrolyte solutions (ITIES) can be employed for energy storage and conversion, solvent extraction, or sensing or in life sciences. Among them are catalytic reactions, which have only been recently studied. Here H_2O_2 generation is studied with decamethylferrocene (DMFc) as electron donor at the interface between tetrahexylammonium perchlorate solution in 1,2-dichloroethane (1,2-DCE) and aqueous $HClO_4$. These conditions are unfavorable for proton transfer across ITIES because of positive Galvani potential difference. Voltammetry with 1,2-DCE droplet modified electrode shows that DMFc oxidation is accompanied by ClO_4^- insertion into the organic phase. The reaction progress was followed by UV−vis spectroscopy, voltammetry, and scanning electrochemical microscopy (SECM). In the first and last method, horseradish peroxidase was used as catalyst. It is concluded that O_2 is reduced to H_2O_2 at the liquid|liquid interface not only under conditions when proton transfer to organic phase is strongly favored, namely, when Galvani potential difference is negative (*Angew. Chem., Int. Ed.* **2008**, *47*, 4675−4678).

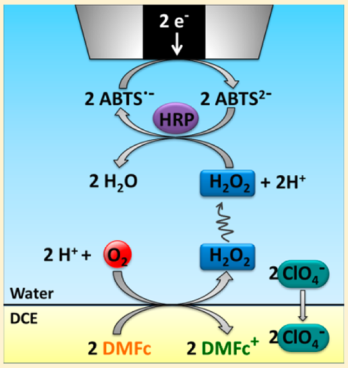

INTRODUCTION

Catalysis at interfaces between two immiscible electrolyte solutions (ITIES) has recently gained increased interest.[1] This is because at soft interfaces a wide range of charge transfer processes such as simple or assisted ion transfer, electron transfer, or proton assisted electron transfer can be driven by polarization of ITIES, namely, Galvani potential difference. It can be generated by applying voltage across ITIES or more practically, by appropriate selection of electrolytes having a common ion in both phases.[2] In a typical case, the substrates and the products are present in one phase, whereas the electron donor is present in the other one.[3]

Oxygen reduction to H_2O_2 is the most frequently studied catalytic reaction at soft interfaces.[4] It is worth mentioning that hydrogen peroxide is an important product because of its consumption by industry on the level of 2.2 million tons per annum.[5] The construction of fuel cell generating hydrogen peroxide is also an interesting concept from the point of view of its economy.[6] Metal porphyrins, tetrathiafulvalene, tetrachlorohydroquinone, and ferrocene derivatives such as decamethylferrocene (DMFc) or 1,2-diferrocenylethane were used as electron donors in oxygen reduction to hydrogen peroxide at polarized 1,2-dichloroethane (DCE)|water (W) interfaces.[1,4,6−13] This reaction was proposed to involve proton transfer from aqueous (W) to organic phase (O) followed by O_2 reduction to H_2O_2 formed in the aqueous phase with both oxidized and reduced forms of DMFc remaining in organic phase:[1]

$$O_{2(W)} + 2DMFc_{(O)} + 2H^+_{(W)} \rightarrow H_2O_{2(W)} + 2DMFc^+_{(O)} \tag{1}$$

DMFc molecules serve as a source of electrons and formation of their protonated form, $DMFcH^+$, is the first step of this reaction. In earlier reports, this reaction was carried out under conditions favorable for proton transfer.[4] This was achieved by application of extremely hydrophobic electrolyte, that is, bis(triphenylphosphoranylidene)ammonium tetrakis(pentafluorophenyl)borate in the organic phase and the hydrophilic lithium salt of the same anion in the aqueous phase to keep the Galvani potential difference ($\Delta_W^{DCE}\phi$) lower than the proton transfer standard potential ($\Delta_W^{DCE}\phi^\circ_{H^+}$).

Here we show that H_2O_2 is generated from oxygen at polarized DCE|W interface also when proton transfer is unfavorable, that is, when $\Delta_W^{DCE}\phi$ is higher than $\Delta_W^{DCE}\phi^\circ_{H^+} = -0.55$ V.[14] This is achieved with ClO_4^- anions present in both phases. Taking into account $\Delta_W^{DCE}\phi^\circ_{ClO_4^-} = 0.177$ V[15] and assuming the same activities of ClO_4^- in both phases, a general expression for Galvani potential difference,

Received: June 28, 2013
Revised: September 6, 2013
Published: September 10, 2013

$$\Delta_{W}^{DCE}\phi = \Delta_{W}^{DCE}\phi^{0}_{ClO_4^-} + \frac{RT}{F}\ln\frac{a_{ClO_4^-}(DCE)}{a_{ClO_4^-}(W)} \tag{2}$$

can be rewritten to give

$$\Delta_{W}^{DCE}\phi = \Delta_{W}^{DCE}\phi^{0}_{ClO_4^-} = 0.177V \tag{3}$$

Clearly, under these conditions, $\Delta_W^{DCE}\phi$ is higher than $\Delta_W^{DCE}\phi^0_{H^+}$ and proton transfer is unfavorable.

This report starts from voltammetric experiments with glassy carbon (GC) electrode covered with droplet of supported organic phase containing DMFc immersed in a wide range of aqueous electrolytes.[16] This was done to estimate to what extent generation of DMFc$^+$ in the organic phase (reaction 1) results in expulsion of electron donor from the organic phase or anion insertion into the organic phase. Generation of H_2O_2 under conditions unfavorable for proton transfer was monitored by change of solution color[17,18] or scanning electrochemical microscopy (SECM). The latter methods allows detection of electroactive molecules close to ITIES.[19,20] Here, for the first time SECM enzymatic detection of H_2O_2 at the liquid|liquid interface with horseradish peroxidase (HRP) is reported. Here, the ability of HRP to catalyze two-electron hydrogen peroxide reduction to water[21,22] with 2,2′-azino-bis-3-ethylbenzothiazoline-sulfonate (ABTS^{2-})[17,23−25] as electron donor is employed, because the oxidized form of the mediator can be easily detected at SECM tip.[26] Finally, the possibility of regeneration of DMFc electron donor close to ITIES was studied with two microelectrodes facing each other with ITIES in between.

EXPERIMENTAL METHODS

Chemicals. DMFc (99%) was obtained from ABCR. Tetrahexylammonium perchlorate (THxAP) was prepared by metathesis of tetrahexylammonium chloride (Fluka, 96%) and $HClO_4$ (Sigma-Aldrich, 70%) following the procedure described for tetrabutylammonium perchlorate[27] and recrystallized twice from a mixture of ethyl acetate and ethanol. $NaClO_4$ was purchased from Fluka. ABTS$(NH_4)_2$, HRP type VI-A, NaCl, and DCE were from Sigma-Aldrich. NaH_2PO_4 and NaOH (POCH) were used for 0.1 mol dm^{-3} phosphate buffer (pH 7) preparation. All aqueous solutions were prepared with demineralized and filtered water from ELIX system (Millipore). Argon gas was from Multax.

Apparatus and Procedures. Cyclic voltammetry and square wave voltammetry (SWV) with GC modified with the organic droplet were performed with Autolab (Eco Chemie) electrochemical workstation. Interfacial reaction was performed through 24 h with stirring. The volumes of DCE and W phases were 2 mL each, and internal diameter of the flasks was 13 mm. Pt disk microelectrode (10 μm diameter, nLab) or GC (2 mm diameter, nLab) were used as working electrodes. Pt wire was used as counter electrode; Ag wire or Ag/AgCl/KCl were used as reference electrodes.

SECM measurements were carried out with CHI900B SECM workstation (CH Instruments). Pt microelectrodes for SECM experiments were made by sealing a Pt wire (25 μm diameter, Goodfellow, England, or 100 μm diameter, Mennica Polska, Poland) using PC-10 micropipet puller (Narishige) into borosilicate glass capillaries and polished. These microelectrodes were used as working electrodes in aqueous and organic solution, respectively. The microelectrode immersed in organic phase was fixed upward at the bottom of the cell. Pt wire and Ag/AgCl/KCl were counter and reference electrodes respectively, and were immersed in the aqueous phase. The Ag|AgCl|KCl electrode had an additional glass compartment with a frit filled with 0.1 mol dm^{-3} aqueous $HClO_4$ perchloric acid solution to prevent traces of Cl$^-$ anions from transferring to the cell. This is important, because of their possible oxidation on the Pt at potentials above 1.1 V vs Ag/AgCl/KCl. The Pt microelectrode in the aqueous phase served as SECM tip, and its position was controlled by stepper motors in the *X*, *Y*, and *Z* directions. A specwell 10 × 30 monocular precision magnifier was used to confirm the distance between two electrodes. All working electrodes were polished with 1, 0.3, and 0.05 μm alumina and sonicated in demineralized water. Argon was bubbling through the two liquid phases for 15 min before measurements, and during the measurement, it was passed above the solution. UV−vis spectra were recorded by Evolution 300 UV−vis spectrophotometer, Thermo Scientific. All measurements were performed at room temperature (22 ± 2 °C).

RESULTS AND DISCUSSION

Voltammetry and SECM with Droplet Modified Electrode. Voltammetry and SECM were used as diagnostic tools to determine the mechanism of ion transfer reaction following DMFc$^+$ cation formation. This is an important aspect of the mechanism of H_2O_2 generation at ITIES. First, cyclic voltammetry was performed on GC electrode modified with droplet of DMFc solution in THxAP supported DCE immersed in a wide range of aqueous electrolytes, including these containing ClO_4^- anions (Figure 1).

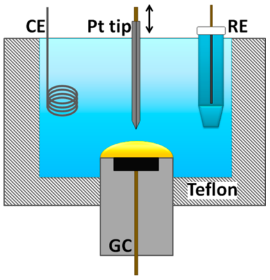

Figure 1. A scheme of the electrochemical cell used in the voltammetric and SECM measurements with droplet modified GC electrode.

The anodic and cathodic peaks on the voltammograms in Figure 2 are due to one electron oxidation of DMFc and reduction of DMFc$^+$, respectively. It is clear that the position of voltammetric oxidation−reduction signal on the potential axis depends on the type of anion. Namely, the midpeak potential, E_{mp}, is negatively shifted in the presence of more hydrophobic anions.

In order to maintain electroneutrality, reversible electrochemical oxidation of DMFc can be followed by anion insertion into DCE,

$$DMFc_{(DCE)} + An^-_{(W)} \rightleftarrows DMFc^+_{(DCE)} + An^-_{(DCE)} + e^- \tag{4}$$

or organic electrolyte cation, THxA$^+$, expulsion from DCE into the aqueous phase,

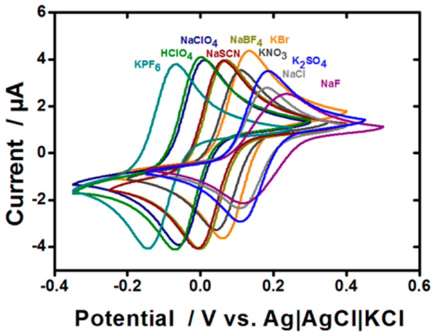

Figure 2. Cyclic voltammograms recorded at the GC electrode immersed in 0.1 mol dm^{-3} aqueous solution of various salts. The GC electrode was covered with 2 μL of 1 mmol dm^{-3} DMFc solution in 0.1 mol dm^{-3} THxAP in DCE. Scan rate = 50 mV s^{-1}.

$$\mathrm{DMFc}_{(\mathrm{DCE})} + \mathrm{THxA}^{+}_{(\mathrm{DCE})} \rightleftarrows \mathrm{DMFc}^{+}_{(\mathrm{DCE})} + \mathrm{THxA}^{+}_{(\mathrm{W})} + \mathrm{e}^{-} \quad (5)$$

or expulsion of newly formed DMFc$^+$ cation from DCE into the aqueous phase,

$$\mathrm{DMFc}_{(\mathrm{DCE})} \rightleftarrows \mathrm{DMFc}^{+}_{(\mathrm{W})} + \mathrm{e}^{-} \quad (6)$$

Almost constant magnitude of anodic and cathodic peak currents in the subsequent voltammetric scans is noted in the experiments performed in aqueous electrolyte containing ClO$_4^-$. This indicates no decrease of DMFc concentration in DCE deposit, pointing out reactions 4 or 5. On the other hand, in the experiment performed in the aqueous NaCl, as an example of an electrolyte with a more hydrophilic anion than ClO$_4^-$, a significant decrease of voltammetric current is seen (Supporting Information, Figure S2) indicating DMFc$^+$ expulsion (reaction 6).

Here, as a diagnostic criterion for anion insertion reaction (reaction 4), the following Nernst type equation can be applied:[16]

$$E_{\mathrm{mp}} = E^{\circ}_{\mathrm{DMFc^+/DMFc}} + \Delta_{\mathrm{W}}^{\mathrm{DCE}}\phi^{\circ}_{\mathrm{An^-}} - \frac{RT}{F}\ln c_{\mathrm{An^-(W)}} + \frac{RT}{F}\ln\frac{c^{*}_{\mathrm{DMFc}}}{2} \quad (7)$$

where $\Delta_{\mathrm{W}}^{\mathrm{DCE}}\phi^{\circ}_{\mathrm{An^-}}$ is the standard potential of anion transfer from W to DCE, $c_{\mathrm{An^-(W)}}$ is the concentration of anions in the aqueous phase, and c^{*}_{DMFc} is the concentration of DMFc in DCE. It predicts unity slope of E_{mp} vs $\Delta_{\mathrm{W}}^{\mathrm{DCE}}\phi^{\circ}_{\mathrm{An^-}}$ dependence if reaction 4 occurs, whereas zero slope is expected for reactions 5 and 6. Equation 7 also predicts −59 mV/dec slope of logarithmic anion concentration dependence for reaction 4. In the absence of anion insertion (reactions 5 and 6), zero slope is expected.

Here, for more hydrophobic anions linear dependence of E_{mp} vs $\Delta_{\mathrm{W}}^{\mathrm{DCE}}\phi_{\mathrm{An^-}}$ is seen with a slope of 0.6 (Figure 3). This effect is even more clear when a larger number of data is analyzed using literature values of standard transfer potentials for nitrobenzenelwater ($\Delta_{\mathrm{W}}^{\mathrm{NB}}\phi$) systems (Supporting Information, Figure S1). Moreover, the slope of the dependence of the peak potential, E_{p} (obtained from SWV experiments), on the logarithm of ClO$_4^-$ concentration in the aqueous phase is equal to −59 mV/dec These results, together with stability of voltammograms (Supporting Information, Figure S2) point to ClO$_4^-$ insertion (reaction 4). The expulsion of THxA$^+$ cations to aqueous solution can be ruled out because the transfer potential of THxA$^+$, $\Delta_{\mathrm{W}}^{\mathrm{DCE}}\phi^{\circ}_{\mathrm{THxA^+}}$ = 0.470 V[28,29] is much higher than $\Delta_{\mathrm{W}}^{\mathrm{DCE}}\phi^{\circ}_{\mathrm{ClO_4^-}}$ = 0.177 V.[15]

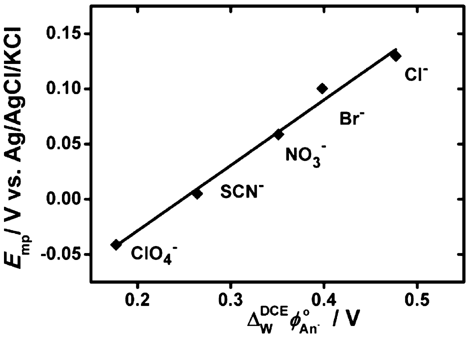

Figure 3. Dependence of the midpeak potential of the DMFc$^+$/DMFc couple, E_{mp}, on the standard transfer potential of the studied anions,$\Delta_{\mathrm{W}}^{\mathrm{DCE}}\phi_{\mathrm{An^-}}$[16] obtained from the data presented in Figure 2.

The slope of −21 mV/dec of E_{p} vs logarithm of Cl$^-$ concentration dependence indicates significant contribution of cation expulsion. The instability of voltammograms (Supporting Information, Figure S2) indicates that DMFc$^+$ is expelled from the DCE drop. However, similar values of transfer potential of Cl$^-$ anion ($\Delta_{\mathrm{W}}^{\mathrm{DCE}}\phi^{\circ}_{\mathrm{CL^-}}$ = 0.477 V[15]) and THxA$^+$ cation ($\Delta_{\mathrm{W}}^{\mathrm{DCE}}\phi^{\circ}_{\mathrm{THxA^+}}$= 0.470 V[28,29]) indicate that THA$^+$ expulsion is also likely to occur.

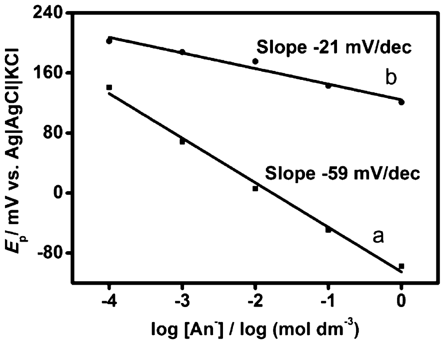

Figure 4. Dependence of the SWV peak potential of DMFc oxidation on the logarithm of ClO$_4^-$ (a) and Cl$^-$ (b) concentration in the aqueous phase. The SWV parameters: step potential 1 mV, frequency 8 Hz, amplitude 50 mV.

In order to detect DMFc$^+$ cations expelled from DCE film, the SECM microelectrode tip (diameter 25 μm) was positioned in front of a liquid modified GC electrode to detect DMFc$^+$ cations (Figure 1).[30] The control of the distance between the tip and ITIES is a crucial point in this experiment. First, the approach curve to the liquid deposit was recorded by applying a potential of 0.2 V to the tip. This potential corresponds to oxidation of DMFc in DCE (Supporting Information, curves a and b in Figure S3). The sharp increase of the current marks penetration of SECM tip into an organic phase ("enter point"). Then the tip movement direction was inverted, and at some position the current drops down indicating that the tip left the organic phase ("exit point") (Supporting Information, Figure S3). The distance between the "enter point" and "exit point' equals ca. 300 μm, perhaps due to hydrophobic DCE drop distortion caused by pushing and pulled out the hydrophilic SECM tip. However, one can assume that after retraction of the tip by the same distance from the "exit point" (20 μm), the tip-to-ITIES distance is always the same.

Then for 100 s potential 0.6 V was applied to DCE-modified GC electrode to produce $DMFc^+$ cations, whereas the SECM tip was kept at potential allowing for their reduction in aqueous phase (−0.6 V). Clearly, from cyclic voltammograms obtained at the tip after deposition, much higher anodic current, corresponding to oxidation of solid DMFc,[31] is observed in aqueous NaCl than in $NaClO_4$ (Figure 5), indicating more efficient expulsion of $DMFc^+$ cations in the presence of chloride ions.

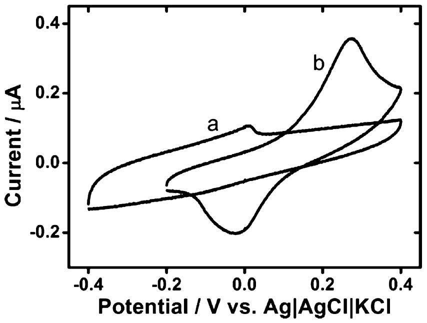

Figure 5. Cyclic voltammograms recorded at the 25 μm diameter Pt microelectrode immersed in 0.1 mol dm^{-3} $NaClO_4$ (a) or NaCl (b) aqueous solution after 100 s of deposition. The Pt electrode was placed in front of the GC electrode (Figure 1) coated with 30 μL of 5 mmol dm^{-3} DMFc solution in 0.1 mol dm^{-3} THxAP in DCE. The GC electrode potential was 0.6 V. Scan rate 15 V s^{-1}.

One can roughly estimate the concentration of $DMFc^+$ in the volume between the tip and organic phase ($C°$) from the following equation:[32]

$$C° = \frac{Q}{4nFDrt} \tag{8}$$

where Q is the anodic peak charge integrated from CV recorded after deposition, n is the number of electrons transferred per molecule, F is the Faraday constant, $D = 1 \times 10^{-5}$ cm^2 s^{-1} is the diffusion coefficient of $DMFc^+$ (its value was obtained in dichloromethane[33]), r is the SECM tip radius, and t is the time of electrolysis.[32] This concentration is 1 order of magnitude smaller in aqueous $NaClO_4$ solution (2.1×10^{-8} mol dm^{-3}) than in NaCl solution (1.1×10^{-7} mol dm^{-3}) indicating a smaller contribution of $DMFc^+$ cation expulsion in the latter case.

To summarize, the experiments described above indicate that when DMFc solution in supported DCE is in contact with aqueous electrolyte containing ClO_4^- anions, oxidation of DMFc is followed by anion insertion from the aqueous to the organic phase.

H_2O_2 Generation at ITIES, Visual and Voltammetric Detection. Next, hydrogen peroxide generation at the polarized DCE(THxAP)|W($HClO_4$) interface was studied under aerobic conditions. The yellow solution of DMFc in DCE turns green after its oxidation, indicating formation of $DMFc^+$ cations.[4,6] This is clearly visible after 24 h with different concentrations of DMFc or protons (Figure 6 A, row II). In turn, violet color (Figure 6A, row IV) is seen when KI and starch are added to the aqueous phase, due to the following reaction:[6]

$$3I^- + H_2O_2 + 2H^+ \rightarrow I_3^- + 2H_2O \tag{9}$$

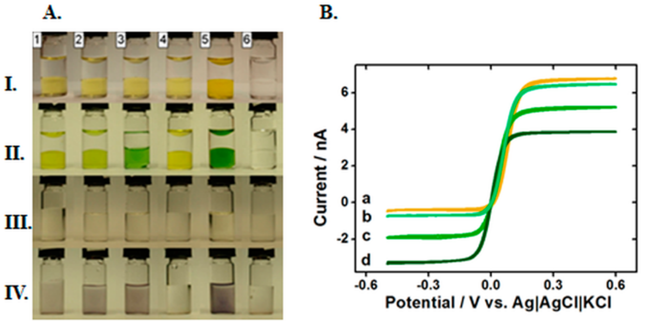

Figure 6. (A) Photographs of the reaction flasks just after solution preparation (row I) and after 24 h of two-phase reaction (row II), of aqueous phase collected after 24 h of two-phase reaction, mixed with 1 mL of 0.1 mol dm^{-3} aqueous KI (row III) and of flasks from row III with 100 μL of 10% starch solution added (row IV). Upper phase (rows I and II) consists of aqueous $HClO_4$ (1, 0.01 mol dm^{-3}; 2, 0.1 mol dm^{-3}; 3, 5, and 6, 0.5 mol dm^{-3}) or 0.5 mol dm^{-3} $NaClO_4$ (4, control experiment). The lower phase contains various concentrations of DMFc in 0.1 mol dm^{-3} THxAP solution in DCE (1−4, 5 mmol dm^{-3}, 5, 50 mmol dm^{-3}). Flasks in column 6 did not contain DMFc (control experiment). (B) Voltammograms recorded in the organic phase at a Pt microelectrode (10 μm diam) immersed in fresh 5 mmol dm^{-3} DMFc in 0.1 mol dm^{-3} THxAP solution in DCE (a) and after contact with 0.01 (b), 0.1 (c), and 0.5 (d) mol dm^{-3} $HClO_4$ for 24 h in aerobic conditions. Scan rate was 20 mV s^{-1}.

These results indicate a similar effect of electron donor and proton concentration on H_2O_2 generation rate. Results of control experiments with sodium perchlorate solution or in the absence of DMFc (Figure 6A, columns 4 and 6) indicate that both protons and electron donor are indispensable for this reaction. The reaction is slower than reported earlier under conditions favoring proton transfer across the liquid|liquid interface.[6] As was shown above, $DMFc^+$ transfer into the aqueous phase is also minor. Taking into account that the value of $\Delta_W^{DCE}\phi^\circ_{ClO_4^-}$ is higher than $\Delta_W^{DCE}\phi^\circ_{THxA^+} = 0.470$ V[28,29] and ${}_W^{DCE}\phi^\circ_{H^+} = -0.55$ V,[14] one can conclude that H_2O_2 generation occurs at the liquid|liquid interface and is accompanied by insertion of ClO_4^- anions into the organic phase:

$$O_2 + DMFc(DCE) + 2H^+_{(W)} + CLO_4^-{}_{(W)} \rightarrow H_2O_{2(W)} + DMFc^+_{(DCE)} + CLO_4^-{}_{(DCE)} \tag{10}$$

The role of the protons in reaction 10 is also confirmed by cyclic voltammetry in the organic phase after 24 h of reaction (Figure 6B). After contact with the organic phase, the cathodic wave corresponding to $DMFc^+$ cation electroreduction appears and its magnitude increases for a larger concentration of $HClO_4$.

Spectroscopic Detection of H_2O_2. Concentration of H_2O_2 generated in the two-phase reaction was estimated by UV−vis spectroscopy after separation of the aqueous phase. For this purpose, HRP-catalyzed reduction of hydrogen peroxide to water in the presence of $ABTS^{2-}$ anion resulting in formation of $ABTS^{\bullet -}$ anion radical,[34]

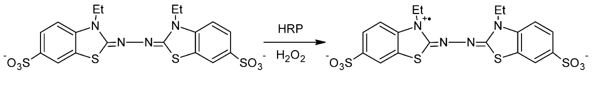

$ABTS^{2-}$ $ABTS^{\cdot -}$ (11)

was employed. The reduced form of mediator exhibits characteristic absorption bands at 416 and 736 nm at pH 7

(Supporting Information, Figure S4). Here, a calibration curve was constructed with acidic solution prepared by mixing 1.4 mL of 0.5 g dm^{-3} HRP and 1.82 mmol dm^{-3} $(NH_4)_2$ABTS solution in 0.1 mol dm^{-3} phosphate buffer (pH 7) with 0.6 mL of 0.5 mol dm^{-3} aqueous $HClO_4$ to keep similar amount of acid as in the flask experiments. A linear dependence of absorbance on concentration was found for H_2O_2 concentration range 0−30 mmol dm^{-3} (Supporting Information, Figure S5). The two phase reaction was performed for 24 h in a glass flask (13 mm inner diameter) with mechanical stirring after mixing 1.5 mL of 0.5 or 5 mmol dm^{-3} DMFc with 0.1 mol dm^{-3} THxAP in DCE and 1.5 mL of 0.5 mol dm^{-3} $HClO_4$ under aerobic conditions. After addition of $(NH_4)_2$ABTS and HRP to 0.6 mL of separated aqueous phase, the H_2O_2 concentration was determined as equal to 15 and 81 μmol dm^{-3} for smaller and larger DMFc concentration, respectively. This is smaller than reported earlier under conditions favorable for proton transfer.[6]

SECM Enzymatic Detection of H_2O_2 at ITIES. Color change caused by mediator reduction can be also observed under quiescent conditions in the biphasic system (Figure 7).

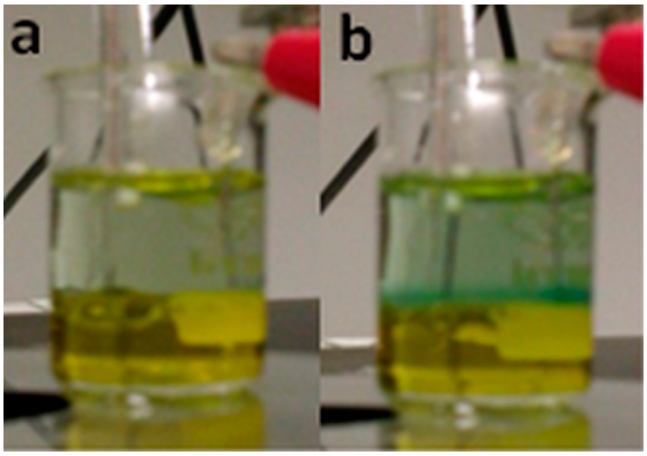

Figure 7. Photos of biphasic systems consisting of 50 mmol dm^{-3} DMFc in 0.1 mol dm^{-3} THxAP in DCE (lower phase) and 0.5 g dm^{-3} HRP, 1.82 mmol dm^{-3} $(NH_4)_2$ABTS in 0.1 mol dm^{-3} aqueous $HClO_4$ (upper phase) just after pouring solutions into the beaker (a) and 30 min later (b).

At the beginning of the experiment, the aqueous phase is slightly green perhaps due to oxidation of some ABTS^{2-} anions by dissolved oxygen. Thirty minutes later intensive green color appears near the ITIES indicating formation of ABTS$^{\bullet-}$ in the aqueous phase close to the liquid|liquid interface. This also shows that HRP is still active at pH 1, which has not been reported earlier. The control experiments in the absence of enzyme do not show any color change near the interface. This excludes the hypothesis about direct oxidation of ABTS^{2-} by DMFc$^+$.

The generation of H_2O_2 next to the liquid|liquid interface was also detected by SECM with the same aqueous phase composition employing electroreduction of ABTS$^{\bullet-}$ generated at ITIES at the tip (Figure 8A). When it is kept at 0.35 V, ABTS$^{\bullet-}$ is reduced (Figure S6 in Supporting Information). Therefore, the cathodic tip current increase seen during its approach to liquid|liquid interface (Figure 8B) confirms H_2O_2 generation. We made also an attempt to estimate its flux assuming fast kinetics of enzymatic reaction 12 (rate constant equals 10^7 mol^{-1} dm^3 s^{-1}[35]). Under such conditions, H_2O_2 is converted to H_2O immediately after its generation at the ITIES. Then, ABTS$^{\bullet-}$ radical anions are generated only in the close vicinity to the interface (surface reaction) and they diffuse linearly from the interface at the same rate that they are generated at steady-state conditions. Concentration gradient of ABTS$^{\bullet-}$ close to ITIES is then proportional to its flux according to the first Fick's law. The approach curve slope ($\partial i/\partial z$), obtained for distances higher than 10 radii of the SECM probe, where feedback effect[20] is excluded, is equal to 152 pA cm^{-1}. It is proportional to the concentration gradient of ABTS$^{\bullet-}$ and corresponds to the flux of ABTS$^{\bullet-}$, 3.15 × 10^{-13} mol cm^{-2} s^{-1}, according to the following equation:

$$J_{\mathrm{ABTS}^{\bullet-}} = \left(\frac{\partial i}{\partial z}\right)\left(\frac{1}{4nFr}\right) \qquad (12)$$

where i is the current and z is the SECM probe vertical position. According to the stoichiometry of the process (Figure 8A), the flux of H_2O_2 is half of the flux of ABTS$^{\bullet-}$, that is, 1.58 × 10^{-13} mol cm^{-2} s^{-1}.

It has to be emphasized that both methods of H_2O_2 detection are not much affected by its partitioning to DCE phase.[6]

Regeneration of DMFc Electron Donor. H_2O_2 generation occurs only when the substrates (O_2 and protons) and electron donor, DMFc, meet at liquid|liquid interface. It seems that the efficiency of this process can be increased by electrochemical regeneration (reduction) of its oxidized form,

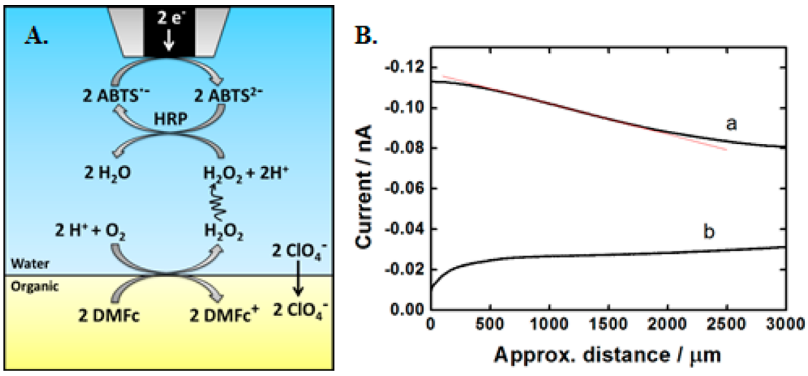

Figure 8. (A) Scheme of SECM experiment for enzymatic detection of H_2O_2 generated at the liquid|liquid interface. (B) Probe approach curves in the same system as shown in panel A and Figure 7 recorded in the presence (a) and absence (b) of HRP. Tip potential (Pt, 25 μm diameter) was 0.35 V, and its velocity was 10 μm s^{-1}.

$DMFc^+$. In order to check whether it is possible, the SECM experiment was carried out with two microelectrodes of relatively large diameter (100 μm, Pt) facing each other on both sides of the liquid|liquid interface (Figure 9; Supporting Information, Figure S7).

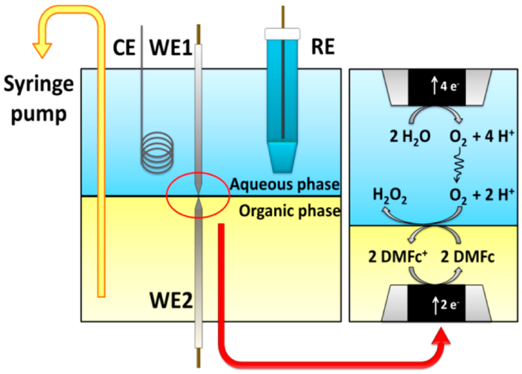

Figure 9. Scheme of the electrochemical cell used for SECM experiment with two microelectrodes close to the liquid|liquid interface.

When microelectrodes are present in separate phases far from the liquid|liquid interface, the voltammogram obtained with WE1 is typical for a platinum electrode in acidic aqueous solution with a characteristic anodic current increase at potentials higher than 1.4 V (Supporting Information, Figure S8), due to water oxidation to O_2. The sigmoidal voltammogram resulting from the redox process of DMFc (Supporting Information, Figure S9) is seen on WE2 immersed in the organic phase, and the half-wave potential of the DMFc/$DMFc^+$ couple was determined to be −0.08 V.

Precise positioning of microelectrodes with respect to ITIES is a crucial point for this experiment. First, in the absence of liquids, fronts of both electrodes were set at almost zero distance with a horizontally aligned optical microscope. Then the WE1 was retracted with exactly known distance (few millimeters), and the cell was filled with DCE electrolyte solution until WE2 was covered. Next, acidic aqueous electrolyte was added. With a syringe pump, the position of the ITIES was set at ca. 66 μm above the WE2 microelectrode utilizing negative feedback of DMFc oxidation under conditions assuring diffusion limiting current[19] (WE2 potential 0.15 V). The liquid interface, hindering DMFc diffusion, was slowly lowered by sucking out the organic phase at a constant flow rate, and the current was recorded (Figure 10). Clearly, it decreases as the distance between WE2 and ITIES decreases. Then the distance was calculated using an equation developed by Cornut and Lefrou[36] (see Supporting Information for details). At $t > 300$ s, the pump was stopped, and ITIES was no longer descending. As a result, steady state current was recorded (Figure 10). This experiment shows that by using a simple stepper motor syringe pump and a syringe with piston diameter much smaller than that of the cell, one can control the position of soft interfaces such as ITIES.

The experimental normalized current (I_T) was calculated as 0.7 from the ratio of the currents recorded at the end and the beginning of experiment. Taking into account the ratio of the insulating glass sheath radius to the radius of the electrode (RG), equal to 4, and the value of normalized heterogeneous rate constant κ, close to 0 (10^{-9}), the distance between the liquid|liquid interface and the front of microelectrode E2 was calculated to be 66 μm.

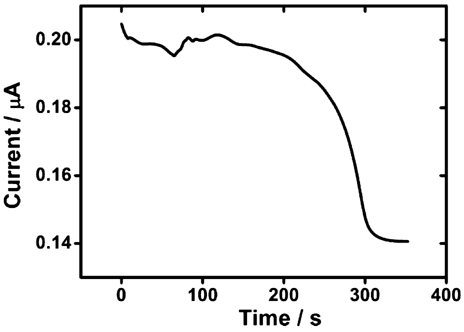

Figure 10. Current−time dependence measured with WE2 electrode at 0.15 V during decreasing the level of organic phase in the cell with setup presented in Figure 9 and Supporting Information, Figure S6.

Then the WE1 electrode was moved back toward the WE2 electrode until the distance between microelectrodes reached 30 μm. The liquid|liquid interface was pushed a bit (ca. 36 μm) by WE1 in such a way that a thin aqueous layer was created on its surface as was earlier observed with a water−nitrobenzene system.[37] The characteristic shape of the CV recorded in these conditions (Supporting Information, Figure S8) confirms that WE1 remained in the aqueous phase. This indicates that SECM scanning at 30 μm WE1−WE2 distance without contact of glass-sealed (hydrophilic) WE2 present in the organic phase with aqueous phase is possible. Further decrease of this distance was impossible, perhaps because of vibrations of the liquid|liquid interface. SECM imaging was performed with current recording at both microelectrodes. The potential of WE1 was set to 1.65 V to produce O_2 by H_2O oxidation.[38] When O_2 reduction to H_2O_2 occurs at the liquid|liquid interface (reaction 10), $DMFc^+$ is produced in the organic phase close to the WE1 surface. This cation is rereduced on WE2 polarized at −0.3 V. Clearly higher cathodic current indicating an excess of $DMFc^+$ was recorded at WE2 when the WE1 tip generating oxygen scanned above WE2 (Figure 11).

This experiment clearly shows regeneration of the electron donor indicating that DMFc may act as a redox catalyst. To confirm that the cathodic current at WE2 is indeed due to reduction of $DMFc^+$ and not due to the reduction of dissolved O_2, we performed a blank experiment without DMFc in DCE.

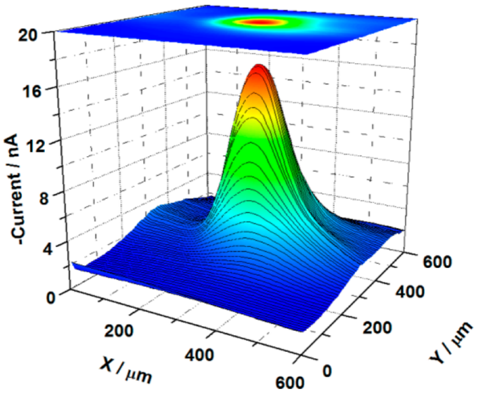

Figure 11. SECM image of $DMFc^+$ reduction at a 100 μm diameter microelectrode in DCE phase. $DMFc^+$ was generated at ITIES by oxygen reduction. O_2 was delivered by water electrolysis at scanning microelectrode. Scanning velocity: 20 μm s^{-1}. See text for details.

Negligible cathodic current indicates no contribution of the latter process, showing a crucial role of DMFc in ORR at the soft interface. Importantly, the collection efficiency, $\Theta = 2I_S/I_T$ (where I_s and I_T denote current recorded on WE2 and WE1, respectively, and the 2 factor is because generation of a single O_2 molecule by water electrolysis requires four electrons contrary to two electrons required for its reduction to H_2O_2) depends on the tip position (Figure S10 in Supporting Information) in a similar way as the WE2 current (Figure 10).

■ CONCLUSIONS

This work shows that H_2O_2 can be successfully generated at ITIES polarized by ClO_4^- as a common ion in both phases. Under such conditions, proton transfer is unfavorable and two-electron oxygen reduction occurs at the liquid|liquid interface. Although the reaction efficiency is smaller than in conditions favorable for proton transfer,[1,3,4,6] this finding will allow us to use more available and less expensive electrolytes both in the organic and in the aqueous phase. Additionally, new methodology of H_2O_2 monitoring close to the liquid|liquid interface, based on scanning electrochemical microscopy and enzymatic reaction, was proposed. In our opinion, it can be applied to other interfaces such as solid|liquid interface. We also presented a method for increasing the efficiency of reaction by electrochemical regeneration of the electron donor. This gives new opportunities to reduce its amount as well as the volume of the organic phase, for example, droplets immobilized on the electrode surface[16,39−41] where small amount of catalyst can be regenerated electrochemically.

■ ASSOCIATED CONTENT

Ⓢ Supporting Information

Additional plots, voltammograms, spectra, and equations. This material is available free of charge via the Internet at http://pubs.acs.org.

■ AUTHOR INFORMATION

Corresponding Author

*Mailing address: Institute of Physical Chemistry, Polish Academy of Sciences, Kasprzaka 44/52, 01-224 Warsaw, Poland. Telephone: +48343-7533. E-mail: mopallo@ichf.edu.pl.

Author Contributions

The manuscript was written through contributions of all authors. All authors have given approval to the final version of the manuscript.

Notes

The authors declare no competing financial interest.

■ ACKNOWLEDGMENTS

This research was supported by Polish-Swiss Research Programme, Project PSPB-035/2010: "Electrocatalysis at droplets". Wojciech Nogala acknowledges NanOtechnology Biomaterials and aLternative Energy Source for ERA Integration [FP7-REGPOT-CT-2011-285949-NOBLESSE] Project from European Union.

■ REFERENCES

(1) Mendez, M.; Partovi-Nia, R.; Hatay, I.; Su, B.; Ge, P.; Olaya, A.; Younan, N.; Hojeij, M.; Girault, H. Molecular electrocatalysis at soft interfaces. *Phys. Chem. Chem. Phys.* **2010**, *12*, 15163−15171.

(2) Volkov, A.; Deamer, D.; Tanelian, D.; Markin, V. *Liquid Interfaces in Chemistry and Biology*; Wiley: New York, 1998.

(3) Partovi-Nia, R.; Su, B.; Li, F.; Gros, C. P.; Barbe, J.-M.; Samec, Z.; Girault, H. Proton Pump for O_2 Reduction Catalyzed by 5,10,15,20-tetra- phenylporphyrinatocobalt(II). *Chem.—Eur. J.* **2009**, *15*, 2335−2340.

(4) Su, B.; Hatay, I.; Ge, P. Y.; Mendez, M.; Corminboeuf, C.; Samec, Z.; Ersoz, M.; Girault, H. Oxygen and proton reduction by decamethylferrocene in non-aqueous acidic media. *Chem. Commun.* **2010**, *46*, 2918−2919.

(5) Hage, R.; Lienke, A. Applications of Transition-Metal Catalysts to Textile and Wood-Pulp Bleaching. *Angew. Chem., Int. Ed.* **2006**, *45*, 206−222.

(6) Su, B.; Partovi-Nia, R.; Li, F.; Hojeij, M.; Prudent, M.; Corminboeuf, C.; Samec, Z.; Girault, H. H_2O_2 generation by decamethylferrocene at a liquid|liquid interface. *Angew. Chem., Int. Ed.* **2008**, *47*, 4675−4678.

(7) Cunnane, V.; Geblewicz, G.; Schiffrin, D. Electron and ion transfer potentials of ferrocene and derivatives at a liquid|liquid interface. *J. Electrochim. Acta* **1995**, *40*, 3005−3014.

(8) Trojanek, A.; Langmaier, J.; Su, B.; Girault, H.; Samec, Z. Electrochemical evidence of catalysis of oxygen reduction at the polarized liquid−liquid interface by tetraphenylporphyrin monoacid and diacid. *Electrochem. Commun.* **2009**, *11*, 1940−1943.

(9) Hatay, I.; Su, B.; Mendez, M.; Corminboeuf, C.; Khoury, T.; Gros, C.; Bourdillon, M.; Meyer, M.; Barbe, J.-M.; Ersoz, M.; Zalis, S.; Samec, Z.; Girault, H. Oxygen reduction catalyzed by a fluorinated tetraphenylporphyrin free base at liquid/liquid interfaces. *J. Am. Chem. Soc.* **2010**, *132*, 13733−13741.

(10) Su, B.; Hatay, I.; Trojanek, A.; Samec, Z.; Khoury, T.; Gros, C.; Barbe, J.-M.; Daina, A.; Carrupt, P.-A.; Girault, H. Molecular electrocatalysis for oxygen reduction by cobalt porphyrins adsorbed at liquid/liquid interfaces. *J. Am. Chem. Soc.* **2010**, *132*, 2655−2662.

(11) Trojánek, A.; Mareček, V.; Jänchenová, H.; Samec, Z Molecular electrocatalysis of the oxygen reduction at a polarized interface between two immiscible electrolyte solutions by Co(II) tetraphenylporphyrin. *Electrochem. Commun.* **2007**, *9*, 2185−2190.

(12) Hatay, I.; Su, B.; Li, F.; Mendez, M.; Khoury, T.; Gros, C.; Barbe, J.-M.; Ersoz, M.; Samec, Z.; Girault, H. Proton-coupled oxygen reduction at liquid|liquid interfaces catalyzed by cobalt porphine. *J. Am. Chem. Soc.* **2009**, *131*, 13453−13459.

(13) Ohde, H.; Maeda, K.; Yoshida, Y.; Kihara, S. Redox reactions between molecular oxygen and tetrachlorohydroquinone at the water|1,2-dichloroethane interface. *J. Electroanal. Chem.* **2000**, *483*, 108−116.

(14) Hatay, I.; Su, B.; Li, F.; Partovi-Nia, R.; Vrubel, H.; Hu, X.; Ersoz, M.; Girault, H. Hydrogen Evolution at Liquid−Liquid Interfaces. *Angew. Chem., Int. Ed.* **2009**, *48*, 5139−5142.

(15) Czapkiewicz, J.; Czapkiewicz-Tutaj, B. Relative Scale of Free Energy of Transfer of Anions. *J. Chem. Soc., Faraday Trans. I* **1980**, *76*, 1663−1668.

(16) Komorsky-Lovric, S.; Lovric, M.; Scholz, F. Cyclic voltammetry of decamethylferrocene at the organic liquid aqueous solution graphite three-phase junction. *J. Electroanal. Chem.* **2001**, *508*, 129−137.

(17) Kadnikova, E. N.; Kostic, N. Oxidation of ABTS by hydrogen peroxide catalyzed by horseradish peroxidase encapsulated into sol − gel glass. Effects of glass matrix on reactivity. *J. Mol. Catal. B: Enzym.* **2002**, *18*, 39−48.

(18) Lindgren, A.; Ruzgas, T.; Gorton, L.; Csoregi, E.; Ardila, G.; Sakharov, I.; Gazaryan, I. Biosensors based on novel peroxidases with improved properties in direct and mediated electron transfer. *Biosens. Bioelectron.* **2000**, *15*, 491−497.

(19) *Scanning Electrochemical Microscopy*; Bard, A., Mirkin, M., Eds.; Taylor & Francis Group: New York, 2012.

(20) Li, F.; Su, B.; Salazar, F.; Partovi-Nia, R.; Girault, H. Detection of hydrogen peroxide produced at a liquid/liquid interface using scanning electrochemical microscopy. *Electrochem. Commun.* **2009**, *11*, 473−476.

(21) Morales, A.; Cespedes, F.; Munoz, J.; Martinez-Fabregas, E.; Alegret, S. Hydrogen peroxide amperometric biosensor based on a biocomposite. *Anal. Chim. Acta* **1996**, *332*, 131−138.

(22) Yu, J.; Ju, H. Preparation of porous titania sol-gel matrix for immobilization of horseradish peroxidase by a vapor deposition method. *Anal. Chem.* **2002**, *74*, 3579−3583.

(23) Cheng, X.; Challier, L.; Etcheberry, A.; Noel, V.; Perez, H. The ABTS-HRP System as an Alternative Method to RRDE for the Determination of the Selectivity of the Oxygen Reduction Reaction. *Int. J. Electrochem. Sci.* **2012**, *7*, 6247−6264.

(24) Childs, R.; Bardsley, W. The steady-state kinetics of peroxidase with 2,2′-azino-di-(3-ethyl-benzthiazoline-6-sulphonic acid) as chromogen. *Biochem. J.* **1975**, *145*, 93−103.

(25) Wang, Q.; Kromka, A.; Houdkova, J.; Babchenko, O.; Rezek, O.; Li, M.; Boukherroub, R.; Szunerits, S. Nanomolar Hydrogen Peroxide Detection Using Horseradish Peroxidase Covalently Linked to Undoped Nanocrystalline Diamond Surfaces. *Langmuir* **2012**, *28*, 587−592.

(26) Nogala, W.; Burchardt, M.; Opallo, M.; Rogalski, J.; Wittstock, G. Scanning electrochemical microscopy study of laccase within a sol−gel processed silicate film. *Bioelectrochemistry* **2008**, *72*, 174−182.

(27) House, H.; Feng, E.; Peet, N. Comparison of various tetraalkylammonium salts as supporting electrolytes in organic electrochemical reactions. *J. Org. Chem.* **1971**, *36*, 2371−2375.

(28) Antoine, J. P.; de Aguirre, I.; Janssens, F.; Thyrion, F. Aspects physicochimiques de la catalyse par transfert de phase. *J. Bull. Soc. Chim. Fr.* **1980**, *II*, 207−232.

(29) Olaya, A.; Mendez, M.; Cortes-Salazar, F.; Girault, H. Voltammetric determination of extreme standard Gibbs ion transfer energy. *J. Electroanal. Chem.* **2010**, *644*, 60−66.

(30) Donten, M.; Stojek, Z.; Scholz, F. Electron transfer − ion insertion electrochemistry at an immobilized droplet: Probing the three-phase electrode-reaction zone with a Pt disk microelectrode. *Electrochem. Commun.* **2002**, *4*, 324−329.

(31) Bond, A.; Marken, F. Mechanistic aspects of the electron and ion transport processes across the electrode | solid | solvent (electrolyte) interface of microcrystalline decamethylferrocene attached mechanically to a graphite electrode. *J. Electroanal. Chem.* **1994**, *372*, 125−135.

(32) Shul, G.; Nogala, W.; Zakorchemna, I.; Niedziolka, J.; Opallo, M. Scanning electrochemical microscopy study of ion transfer process across water/2-nitrophenyloctylether interface supported by hydrophobic carbon ceramic electrode. *J. Solid State Electrochem.* **2008**, *12*, 1285−1291.

(33) Goldfarb, D.; Corti, H. Steady-state voltammetric study of the reduction of decamethylferrocenium in dichloromethane at microelectrodes. *J. Electroanal. Chem.* **2001**, *509*, 155−162.

(34) Grotzky, A.; Nauser, T.; Erdogan, H.; Schluter, D.; Walde, P. A Fluorescently Labeled Dendronized Polymer−Enzyme Conjugate Carrying Multiple Copies of Two Different Types of Active Enzymes. *J. Am. Chem. Soc.* **2012**, *134*, 11392−11395.

(35) Smith, A.; Sanders, S.; Thorneley, R.; Burke, J.; Bray, R. Characterization of a haem active-site mutant of horseradish peroxidase, Phe41→Val, with altered reactivity towards hydrogen peroxide and reducing substrates. *Eur. J. Biochem.* **1992**, *207*, 507−519.

(36) Cornut, R.; Lefrou, C. New analytical approximation of feedback approach curves with a microdisk SECM tip and irreversible kinetic reaction at the substrate. *J. Electroanal. Chem.* **2008**, *621*, 178−184.

(37) Barker, A.; Macpherson, J.; Slevin, C.; Unwin, P.. Scanning Electrochemical Microscopy (SECM) as a Probe of Transfer Processes in Two-Phase Systems: Theory and Experimental Applications of SECM-Induced Transfer with Arbitrary Partition Coefficients, Diffusion Coefficients, and Interfacial Kinetics. *J. Phys. Chem. B* **1998**, *102*, 1586−1598.

(38) Eckhard, K.; Schuhmann, W. Localized visualization of O_2 consumption and H_2O_2 formation by means of SECM for the characterization of fuel cell catalyst activity. *Electrochim. Acta* **2007**, *53*, 1164−1169.

(39) Komorsky-Lovric, S.; Lovric, M.; Scholz, F. Square-Wave Voltammetry of Decamethylferrocene at the Three-Phase Junction Organic Liquid/Aqueous Solution/Graphite. *Collect. Czech. Chem. Commun.* **2001**, *66*, 434−444.

(40) Adamiak, W.; Opallo, M. Electrochemical redox processes of fullerene C_{60} and decamethylferrocene dissolved in cast 1,2-dichlorobenzene film in contact with aqueous electrolyte. *J. Electroanal. Chem.* **2010**, *643*, 82−88.

(41) Quentel, F.; Mirceski, V.; L'Her, M.; Mladenov, M.; Scholz, F.; Elleouet, C. Comparative Study of the Thermodynamics and Kinetics of the Ion Transfer Across the Liquid|Liquid Interface by Means of Three-Phase Electrodes. *J. Phys. Chem. B* **2005**, *109*, 13228−13236.